Modeling the Flow Around a Free Circular Obstruction

Prarabdha O. Yonzon[1], Bryce D. Wilkins[2], T.V. Hromadka II[3]

[1] United States Military Academy [2] Carnegie Mellon University [3] Distinguished Professor, United States Military Academy

Introduction

The Computational Engineering Mathematics program at the United States Military Academy has focused on mesh reduction numerical methods, such as the Complex Variable Boundary Element Method (CVBEM), for solving partial differential equations (PDEs) of the Laplace and related types. This poster focuses on performance differences between this method and domain meshing techniques such as the Finite Element Method (FEM).

To understand an instance of this difference, this research models the groundwater flow around a free circular obstruction. For this specific problem, it is assumed that geologic faults formed a barrier to the groundwater flow, as indicated by the black circle in Figure 1. Also shown in this figure are clusters of potential contamination source points. One of the source points is a Leaking Underground Storage Tank (LUST). The green dot represents the hypothetical location where a contaminant has been detected. The purpose of this study is to determine the source tank of the detected contaminant by modeling the groundwater flow regime and back-tracing the associated streamline that goes through the location of detection. This research uses the CVBEM and FEM to identify the source of the contamination by modeling the stream function and tracing the relevant streamline from the point of detection back to one of the candidate source points.

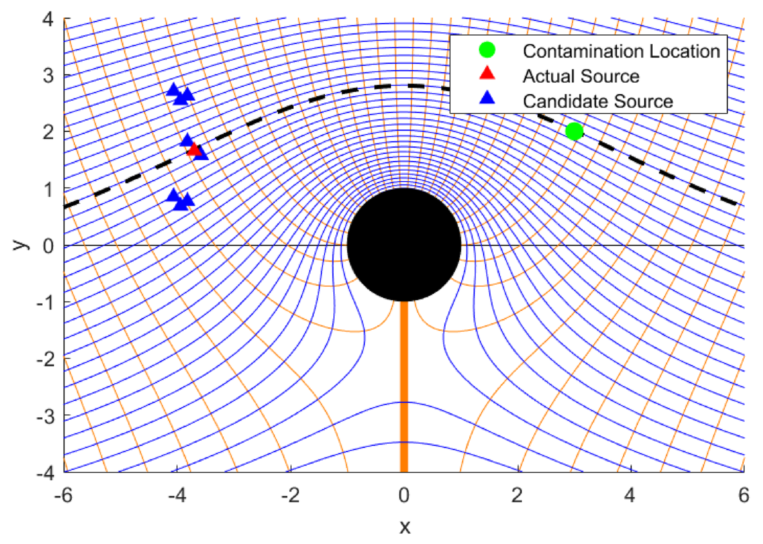

Figure 1: Analytic solution of the groundwater flow. Potential isocontours are depicted as orange lines, and the stream isocontours are shown as blue lines. The analytic solution is given by $\omega(z) = z + \frac{1}{z} + i\frac{3\pi}{4}\log(z)$, as stated in [1].

CVBEM Methodology: Cauchy-Riemann Equations and the CVBEM Approximation Function

The CVBEM approximation function consists of a linear combination of analytic complex variable functions:

$$\hat{\omega}(z) = \sum_{j=1}^{N} c_j g_j(z), \tag{1}$$

where $c_j \in \mathbb{C}$ denotes the complex coefficients; $g_j(z)$ denotes the analytic complex variable basis functions; and N is the number of basis functions being used in the approximation function.

> **NOTE:** There are $2N$ degrees of freedom since each complex coefficient contains an unknown real and imaginary part, which will be determined in the modeling process.

Since the CVBEM approximation function is a linear combination of analytic complex variable functions, the real and imaginary parts of the approximation function are related by the Cauchy-Riemann equations:

$$\frac{\partial \phi}{\partial x} = \frac{\partial \psi}{\partial y} \qquad \frac{\partial \phi}{\partial y} = -\frac{\partial \psi}{\partial x} \tag{2}$$

From Equation (2), it follows that ϕ and ψ are harmonic equations, which satisfy the Laplace equation:

$$\frac{\partial^2 \phi}{\partial x^2} = \frac{\partial^2 \psi}{\partial xy} \quad \text{and} \quad \frac{\partial^2 \phi}{\partial y^2} = -\frac{\partial^2 \psi}{\partial xy} \quad \Longrightarrow \quad \frac{\partial^2 \phi}{\partial x^2} + \frac{\partial^2 \phi}{\partial y^2} = 0 \tag{3}$$

A similar process can be used to show that ψ is also a harmonic function.

Other Important Basis Functions

This work uses basis functions obtained from numerical integration of the Cauchy integral equation, as discussed in [2]:

$$\hat{\omega}(z) = \sum_{j=1}^{N} c_j (z - z_j) \ln\big(z - z_j\big) \tag{4}$$

Other basis functions have been examined in the recent paper [5] and can be seen in the box on the right. These basis functions are complex monomials, a Laurent series expansion, and simple poles, as seen in Equations (5), (6), and (7), respectively.

$$\hat{\omega}(z) = \sum_{j=1}^{N} c_j (z - z_0)^j, \qquad z_0 \in \mathbb{C} \tag{5}$$

$$\hat{\omega}(z) = \sum_{j=1}^{N} c_j \frac{1}{(z - z_1)^j}, \qquad z_1 \in \mathbb{C} \tag{6}$$

$$\hat{\omega}(z) = \sum_{j=1}^{N} c_j \frac{1}{z - z_j} \tag{7}$$

Node Positioning Algorithm and Refinement Procedure

The efficacy of the CVBEM is improved though the use of Node Positioning Algorithms, which are coupled with the CVBEM methodology. The Node Positioning Algorithms of interest can be broadly described in the following six steps:

1. Candidate nodes and candidate collocation points are generated, and the algorithm begins with two selected collocation points.
2. Each candidate node is evaluated to determine the node that corresponds to the CVBEM model of least error. The node with the least maximum error is chosen as the next node for the model.
3. Error is then re-evaluated on the boundary. Two local maxima of the error function are identified, and new collocation points are located at those points, respectively.
4. Steps 2 and 3 are repeated until the required numbers of nodes and collocation points have been selected.
5. Afterwards, each node is re-examined to see if a selection from the remaining candidate nodes would result in a model with a smaller maximum error. If the error is smaller, this node replaces the current node, and the method proceeds to re-evaluate the next node. If the maximum error is not smaller, then the current node is kept, and the next node is evaluated. **This step is known as the refinement procedure and is what distinguishes NPA2 from NPA1.**
6. This refinement continues for a set number of iterations or until the maximum error no longer decreases. Also, note that the refinement procedure can be applied after the selection of each new node in Step 2.

FEM Methodology

The FEM is a common numerical method for solving PDEs that uses a domain discretization consisting of modeling elements and nodes. The figures below show an example of a coarse mesh and a refined mesh.

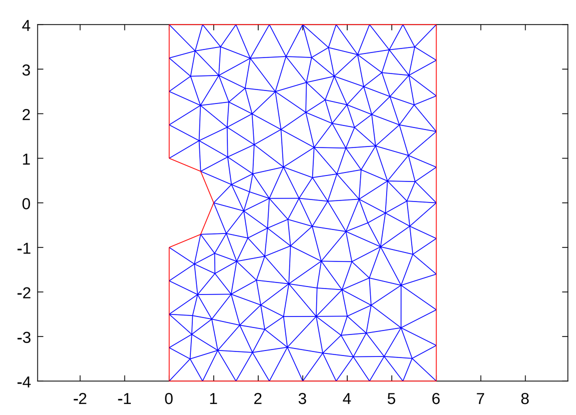

Figure 2: Trial 1 FEM mesh

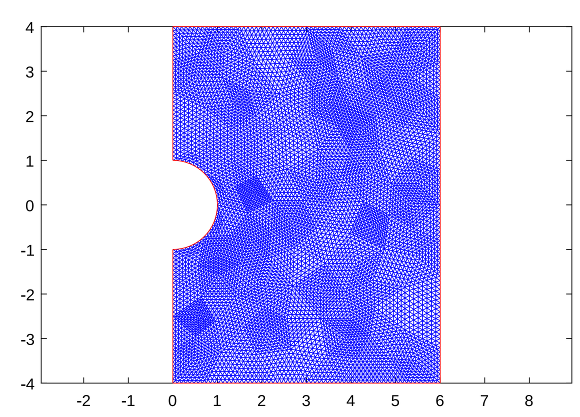

Figure 3: Trial 2 FEM mesh

Refined meshes produce more accurate approximations. This project used the more refined mesh to compare the accuracy of the FEM to the CVBEM.

Results

CVBEM Problem Details and Results

Parameters	Trial 1	Trial 2
Nodes in model:	20	40
Problem Domain Length:	4	4
Problem Domain Height:	8	8
Number of candidate nodes for optimization algorithm:	1000	500
Number of candidate collocation points for optimization algorithm:	2000	1000

Table 1: The Trial 2 parameters were used to produce the CVBEM graphical results displayed below.

Method	Trial 1	Trial 2
NPA1:	3.78×10^{-4}	1.76×10^{-9}
NPA2:	8.63×10^{-6}	1.73×10^{-10}

Table 2: Maximum absolute error comparison for CVBEM models obtained using NPA1 and NPA 2.

Problem Geometry

Symmetry of the problem geometry allows us to justify modeling only the right half of the area of interest, as shown in Figures 4 and 5. Then, these modeling outcomes are reflected about the vertical axis to obtain the approximation in the entire area of interest.

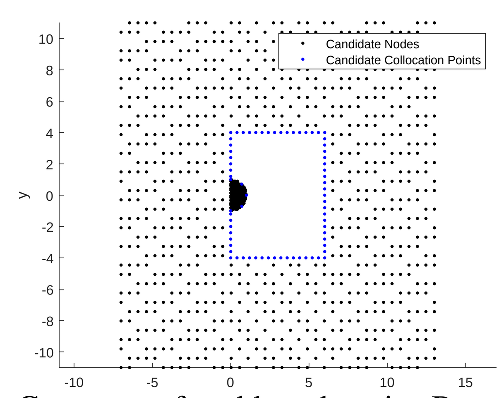

Figure 4: Geometry of problem domain. Boundary conditions are applied at the collocation points. For visualization purposes, only 7% of the candidate collocation points are shown.

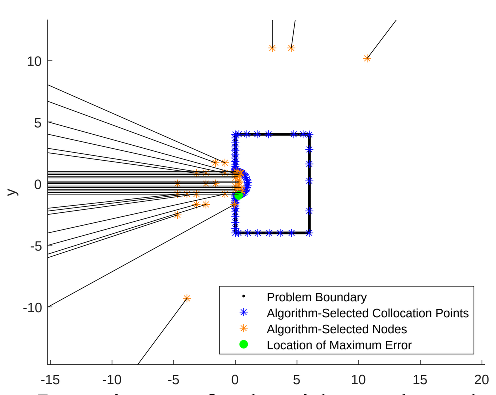

Figure 5: Locations of algorithm-selected collocation points and nodes. The algorithm-selected nodes tend to accumulate in the cavity of the problem domain.

CVBEM Graphical Results

The following figures compare the analytic solution to the CVBEM approximation.

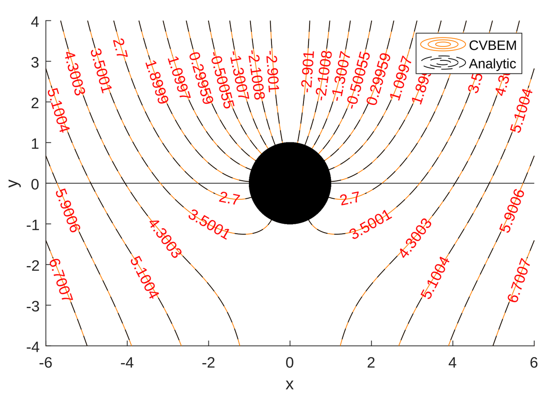

Figure 6: Potential Lines

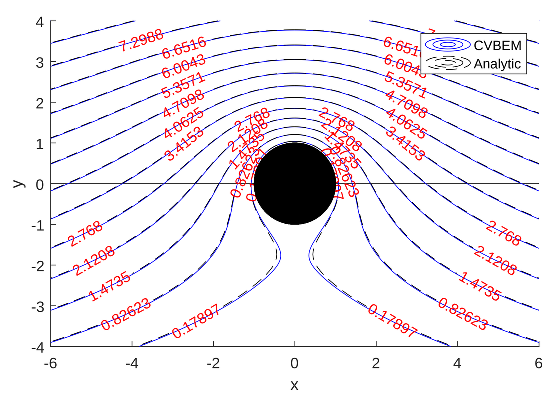

Figure 7: Streamlines

FEM Graphical Results

The following figures compare the analytic solution to the FEM approximation. The figures reveal the FEM streamlines are less accurate than the streamlines produced by the CVBEM.

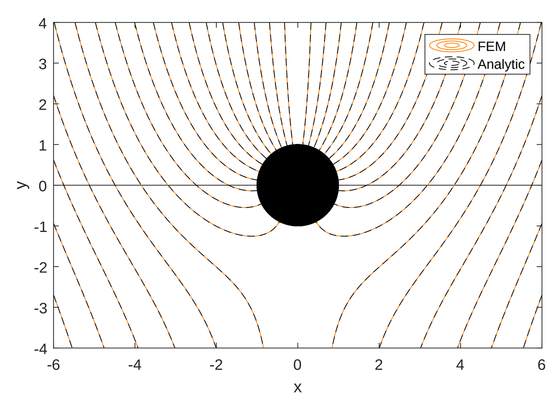

Figure 8: Potential Lines

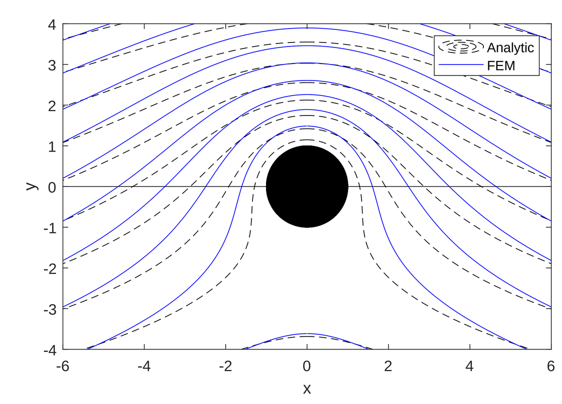

Figure 9: Streamlines

Comparison Between Methods

In this section, we examine the LUST predictions produced by both the CVBEM and FEM methodologies. As shown in Figure 11, the FEM method predicts the incorrect source, while Figure 10 shows the CVBEM predicts the correct source.

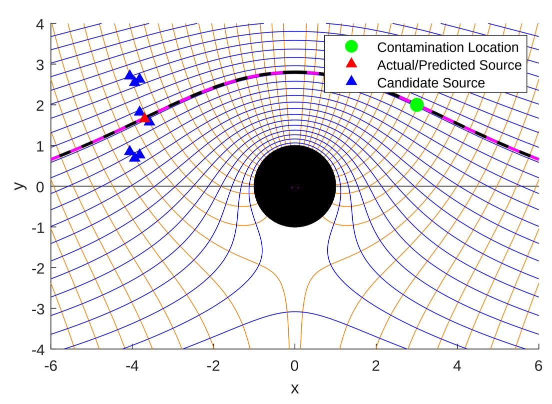

Figure 10: LUST prediction using CVBEM methodology.

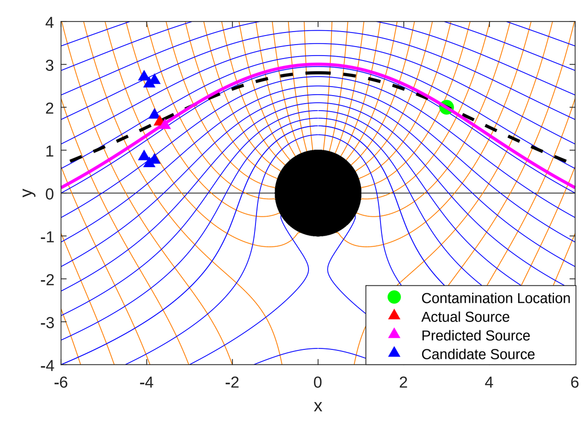

Figure 11: LUST prediction using FEM methodology.

Conclusions

In this research, we analyzed the CVBEM and FEM methods in modeling the flow around a free circular obstruction. We discussed the formulation of the CVBEM approximation function and explained the general idea of the FEM. While comparing the isocontours, we found both methods produced similar isocontours to the analytic ones. However, with more analysis, we found that the FEM model incorrectly identified the source of the contamination. On the other hand, we found that the CVBEM streamlines could be back-traced to correctly identify the source of the contamination.

Acknowledgements

This research was supported by the consulting firm Hromadka & Associates.

References

[1] Kirchhoff, R. H., *Potential Flows Computer Graphic Solutions*. CRC Press, 1985.

[2] Hromadka, T. V. & Guymon, G. L., A complex variable boundary element method: Development. *International Journal For Numerical Methods in Engineering*, **20**, pp. 25–37, 1984.

[3] Wilkins, B. D., Hromadka II, T. V., Johnson, A. N., Boucher, R., McInvale, H. D., Horton, S., Assessment of Complex Variable Basis Functions in the Approximation of Ideal Fluid Flow Problems. *International Journal for Computational Methods and Experimental Measurements*, **7**(1), pp. 45-56, 2019.

[4] Wilkins, B. D., Hromadka II, T. V., McInvale, J., Comparison of Two Algorithms for Locating Computational Nodes in the Complex Variable Boundary Element Method (CVBEM). *International Journal for Computational Methods and Experimental Measurements*, 2020 (in press).

[5] Wilkins, B. D., Hromadka, T. V., Johnson, A. N., Boucher, R., McInvale, H. D. & Horton, S., Assessment of complex variable basis functions in the approximation of ideal fluid flow problems. *International Journal of Computational Methods and Experimental Measurements*, **7(1)**, pp. 45–56, 2019.